AFMR IN $KMnF_3$ NEAR T_N AND T_C; NEW EXPERIMENTAL RESULTS*

By P. Jakubowski

Institute of Physics, Silesian University, Katowice**

(Received November 10, 1977; final version received March 1, 1978)

The AFMR spectra of carefully prepared $KMnF_3$ single crystals have been measured with high temperature resolution near the Néel and Curie temperatures. The results allow several important conclusions: a $KMnF_3$ crystal undergoes structure inversion at temperature $T_X = T_N - 0.5$ K, from tetragonal with $c/a > 1$ to tetragonal with $c/a < 1$; the first-order structural phase transition at $T_S \simeq 81$ K strongly depends on the size of crystallites or crystallographic domains; the Curie temperature T_C cannot be identified with this temperature T_S.

1. Introduction

Since the discovery of weak ferromagnetism in $KMnF_3$ by means of torque measurements [1], the low-temperature structural and magnetic properties of this perovskite-type crystal have been studied very extensively. Experimental work up to date indicates that $KMnF_3$ undergoes a series of structural and magnetic phase transitions. Recent X-ray investigations of its crystal structure were made by Minkiewicz et al. [2] and by Hidaka [3]. Recent neutron diffraction experiments were carried out by Hidaka et al. [4] while the neutron inelastic-scattering experiments were carried out by Gesi et al. [5] and by Shapiro et al. [6]. Raman scattering studies were made by Lockwood and Torrie [7], Lockwood and Coombs [8] and by Eremenko et al. [9]. Ultrasonic attenuation in $KMnF_3$ was measured by Furukawa et al. [10] and recent thermal measurements were carried out by McCormick and Trappe [11] and by Martin et al. [12]. Stress-induced behaviour was examined by Okai and Yoshimoto [13] and by Strauss and Riederer [14]. Magnetic susceptibility has been measured by Maartense and Searle [15] and by Maartense [16]. Finally, the NMR experiments were performed by Borsa [17] and the AFMR experiments by Saiki [18], Saiki et al. [19] and Saiki and Yoshioka [20].

In spite of these extensive studies there remain several very serious problems in our understanding of crystallographic and magnetic behaviour, in particular around the Néel

* Partly supported by the Institute for Low Temperature and Structural Research, Polish Academy of Sciences.

** Address: Instytut Fizyki, Uniwersytet Śląski, Uniwersytecka 4, 40-007 Katowice, Poland.

temperature T_N(88 K) and around the Curie temperature T_C(81 K), where spontaneous weak-ferromagnetism develops.

The purpose of the present work is to reexamine the AFMR results near the temperatures of T_N and T_C with high temperature resolution and by using very carefully prepared single crystals.

2. Experimental procedures

2.1. Specimens

$KMnF_3$ has been studied by the various methods listed in the Introduction. Different methods, of course, require single crystals of different sizes and shapes. Moreover, single crystals can be prepared in several ways. The variety of results reported in the literature probably arises from variations in preparation conditions such as the use of wet and dry methods, different initial temperatures and rates of cooling. Both plastic and elastic deformations at and near the crystal surface due to mechanical damage introduced during lapping, grinding or cutting are closely related to those preparative condition. As Aso pointed out [21], the residual stress induced by lapping, plane-grinding and cutting in an isomorphic $SrTiO_3$ crystal is observable even at a depth larger than 0.1 mm from the damaged face. Hence, for example, the results of optical measurements obtained for an 80 μm thick sample [22] must have without fail a strongly unexpected character. Namely, the large hysteresis observed by Benard and Walker [22] upon warming was almost as large as that observed previously by Beckman and Knox [23], and the same cause in both cases is very probable.

Our samples were obtained from the melt by the modified Bridgman method, according to the procedure described earlier [24]. It should be noted that our $KMnF_3$ single crystals were members of a large class of isomorphic crystals prepared in our laboratory by the same, common, technique; it is very important to know precisely which preparation parameters determine the best quality for the single crystals produced. The AFMR results of $KMnF_3$ were found to be very sensitive to strains, as discussed below, therefore the samples were treated with great precaution. All the samples for AFMR investigations were cloven very carefully with faces parallel to the faces of the cubic-phase unit cell. This can be done easily once the direction and frontal plane of the crystallization of the single-crystal boule is known. All the samples were nearly-cubic parallelepipeds having a volume of about 0.5–1 mm^3. No additional lapping or grinding were needed.

2.2. Measurements

The AFMR measurements of the $KMnF_3$ single crystal have been achieved in the temperature range from 77 to 90 K with the micro-wave frequency of 9.25 GHz. The external field and the oscillating magnetic field made a right angle with each other.

The sample was attached to an aluminium rod which was suspended along the axis of the quartz cold-finger twofold-double-wall Dewar. The calibrated copper-constantan thermocouple was attached to this aluminium rod, in such a manner, however, that the

rod could be rotated along its own axis. The saparation of the thermocouple junction from the sample was 0.5 mm. To limit the thermal coupling between the sample and the environment due to the thermal conductivity of the rod there was an additional liquid--nitrogen container mounted on this rod inside the cryostat.

The temperature resolution is an important aspect in all experiments involving critical phenomena, and it is well known that small sharp features appear in an experiment with a continuously swept temperature rather than in a point by point measurement. In order to obtain the required slow and continuous temperature sweep, both double-wall shields of the cryostat were evacuated to about 10^{-3} Torr and the vacuum was regulated during the experiment. Residual conduction through the shields allowed us to obtain almost any desired rate of temperature sweep. To avoid a hoarfrost on the outside of the cold finger, the resonance cavity was additionally cooled by a flow of cold nitrogen gas. The change in temperature during the analysis of a resonance line in the accurate AFMR measurements was no larger than 0.03 K. The value of absolute temperature was estimated to be correct to within 0.5 K, and the change in the temperature was controlled to within 0.02 K.

When the measurements have been carried out with the applied magnetic field aligned along a cubic axis of the crystal it was believed that the alignment of the crystal in the resonance cavity was correct to within 2°, as deduced from the dependence of the AFMR lines positions on small rotations in the magnetic field.

X-ray examination of the crystal orientation was performed after the AFMR measurements only.

2.3. Preliminary X-ray results

X-ray examination of the crystal quality has been carried out at temperatures from 295 to 125 K by means of the very accurate Bond technique [25]. The results of these investigations indicated that the samples had a preferred orientation which was a result of the growth conditions. It was always the fourfold symmetry axis that was vertical during the crystallization process, while the front of crystallization was nearly parallel to the vertical (110) plane. Below the higher transition at 186 K our samples showed two-domain structure.

3. Resonance equations for uniaxial antiferromagnetic phase

The theoretical formula of the AFMR was obtained by Nagamiya et al. [26]. The resonance equation of the uniaxial antiferromagnetic phase [27] is given by

$$\begin{aligned} &H_p^4 - H_p^2\{H^2[\alpha^2\cos^2\psi + 1] + H_{ef}^2[3\cos^2(\psi-\theta) - 1]\} \\ &- H^2H_{ef}^2[\alpha\cos^2\psi\cos 2(\psi-\theta) + \alpha\cos\psi\sin\theta\sin(\psi-\theta) \\ &+ \sin\psi\cos\theta\sin(\psi-\theta) + (\alpha\cos^2\psi - \sin^2\psi)] \\ &+ H_{ef}^4\cos 2(\psi-\theta)\cos^2(\psi-\theta) + \alpha^2H^4\cos^2\psi = 0, \end{aligned} \tag{1}$$

where we introduced the following notation: $H_p = \omega/\gamma$ is the paramagnetic resonance field, where γ is the gyromagnetic ratio; $H_{ef} = (2H_E H_A)^{1/2}$ is the effective field, where $H_E = \lambda M_i$ is the exchange field and $H_A = K/M_i$ is the axial anisotropy field of the i-th sublattice; H is the applied field which makes an angle θ with the easy axis. The equilibrium direction of sublattice magnetizations defined by the vector $\boldsymbol{m} = \boldsymbol{M}_1 - \boldsymbol{M}_2$ makes an angle ψ with the applied field. α is a coefficient defined by

$$\alpha = 1 - \chi_{\parallel}/\chi_{\perp},$$

where $\chi_{\parallel}$ and $\chi_{\perp}$ represent the susceptibilities parallel and perpendicular to the $\boldsymbol{m}$ direction, respectively. The angles θ and ψ are shown in figure 1, and are related to each other by the relation $\theta - \psi = \eta$. Equation (1) is correct under the assumptions that $H \ll H_E$ (then

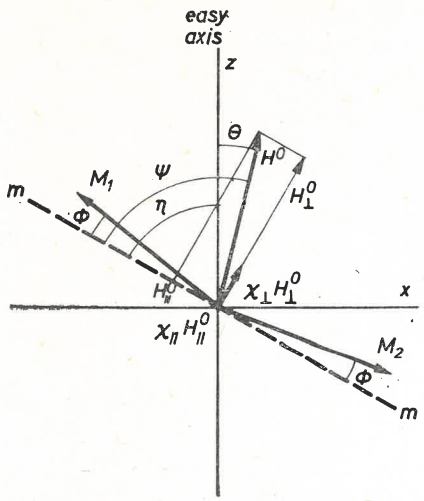

Fig. 1. Balance in the anisotropy field and the definition of the angles from equation (1)

the angle ϕ in figure 1 is negligibly small), $H_A \ll H_E$, and $M_1 = M_2 = M_0$. According to Heeger et al. [28] and to Saiki et al. [19] both these conditions are completely fulfilled.

Let us introduce additional designations as follows

$$H_{ef}^2/H_p^2 = P$$

$$H = \begin{cases} H_{\parallel}\,; \ \theta = \psi = 0 \\ H_{<}\,; \ \theta = \psi = \pi/4 \\ H_{\perp}\,; \ \theta = \psi = \pi/2. \end{cases}$$

Then the AFMR equation (1) takes on the following forms depending on the field orientation $H_{\parallel}$, $H_{<}$ or $H_{\perp}$, and on the value of α

$$H_{\perp} = H_p(1-P)^{1/2}; \qquad \text{any } \alpha \qquad (2a)$$

$$H_{<}^2 = H_p^2(1-P)^2(1-0.5P)^{-1}; \qquad \alpha = 0 \qquad (2b)$$

$$H_{<}^2 = H_p^2\{16.5-4P-16[(1.031-0.25P)^2-0.125(1-P)^2]^{1/2}\}, \quad \alpha = 0.25 \qquad (2c)$$

$$H_{<}^2 = H_p^2\{4.5-4[1.266-0.5(1-P)^2]^{1/2}\}; \quad \alpha = 0.5 \qquad (2d)$$

$$H_{<}^2 = H_p^2\{1.5+0.5P-[0.25(3+P)^2-2(1-P)^2]^{1/2}\}; \quad \alpha = 1 \qquad (2e)$$

$$H_{\parallel} = H_p(1-P); \quad \alpha = 0 \qquad (2f)$$

$$H_{\parallel} = H_p[2.5-0.5(9+16P)^{1/2}]; \quad \alpha = 0.25 \qquad (2g)$$

$$H_{\parallel} = H_p[1.5-(0.25+2P)^{1/2}]; \quad \alpha = 0.5 \qquad (2h)$$

$$H_{\parallel} = H_p - H_{ef}; \quad \alpha = 1. \qquad (2i)$$

All the equations (2a–2i) have two common solutions. The first at $P = 0$, then $H_{\perp} = H_{<} = H_{\parallel} = H_p$, and the second at $P = 1$, then $H_{\perp} = H_{<} = H_{\parallel} = 0$. Accordingly, the AFMR lines arising from different domains should join nominally twice, once at $P = 0$ and again at $P = 1$.

4. AFMR measurements and results

Typical AFMR results, when the applied magnetic field is parallel to the ⟨100⟩ direction, are shown in figures 2 to 5. The Néel temperature is T_N, while T_X is a temperature at which two lines, $H_{\perp}$ and $H_{\parallel}$ (in figure 3, for example) are observed at the same

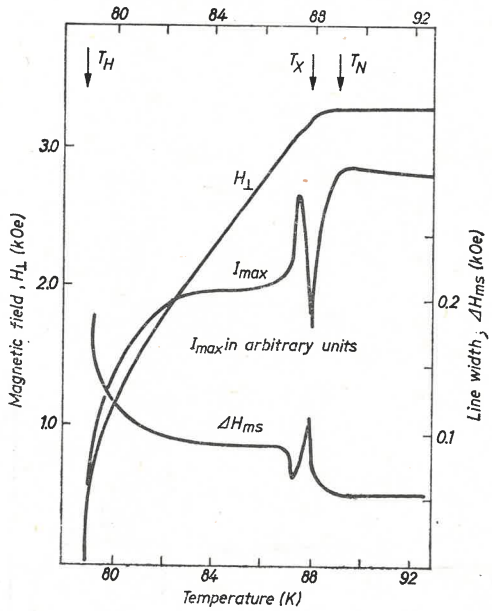

Fig. 2. Temperature dependence of the resonance field $H_{\perp}$ aligned along the ⟨100⟩ direction and perpendicular to the easy axes for both kinds of domains in two-domain single crystal. Corresponding absorption derivative line width ΔH_{ms} and maximal intensity I_{max} are shown versus temperature too. For a definition of the characteristic temperatures T_N, T_X and T_H see the text or the caption of figure 3

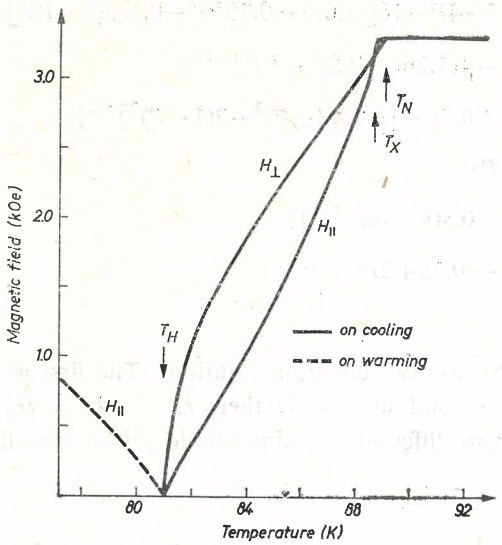

Fig. 3. Temperature dependence of the resonance field when the applied field is aligned along the ⟨100⟩ direction and is perpendicular to the easy axis in one tetragonal domain and parallel to the easy axis in the other. T_N is the Néel temperature, T_X is the temperature of a crossing of the two lines, $H_\perp$ and $H_\parallel$, and T_H is the temperature at which both these lines join at the zero value of the magnetic field

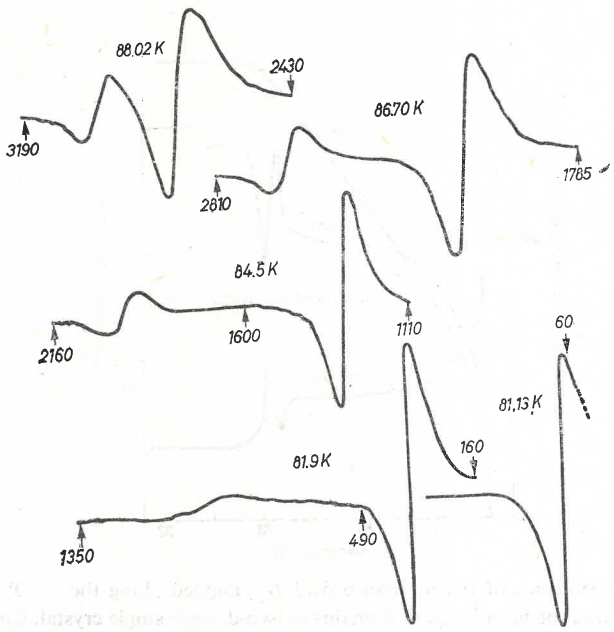

Fig. 4. The AFMR spectra corresponding to the data of figure 3 at various temperatures. The values of the external magnetic field are given in Oe

magnetic field, and T_H is defined as $T_{P=1}$. The AFMR spectra corresponding to figure 3 are shown for some temperatures in figure 4. The near vicinity of the "crossing point", T_X, is displayed more lucidly in figure 5.

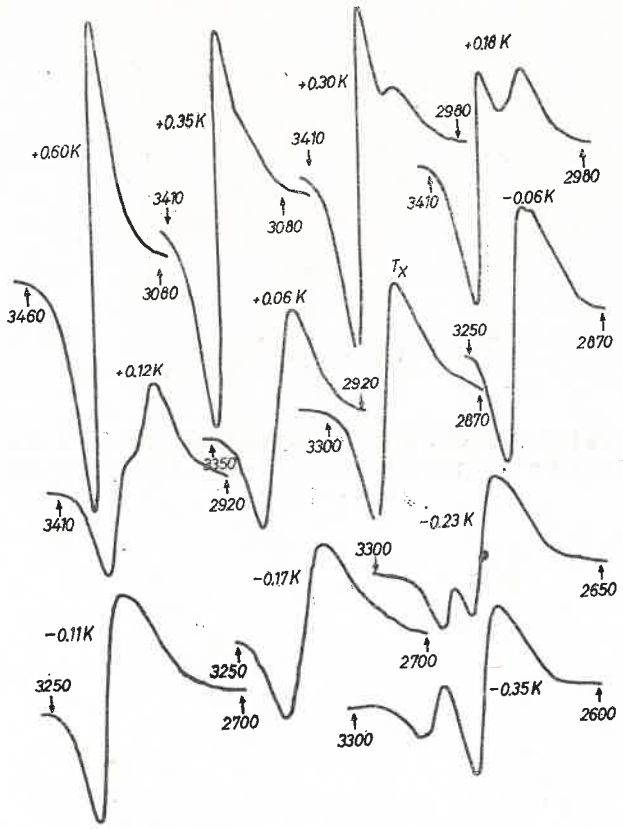

Fig. 5. The AFMR spectra corresponding to the data of figure 3 in the near vicinity of T_X. The values of the external magnetic field are given in Oe

The angular dependence of the resonance fields at 84 K is shown in figure 6. Such a measurement requires a very constant temperature. Because no special temperature stabilization was made, the errors were much larger in this measurement than in any other. The two broken lines in figure 6 approximate the angular dependence of the resonance field evaluated for $\alpha = 0$ and $\alpha = 0.25$ by means of equations (2).

Behaviour of the type displayed in figures 2 and 3 was completely reversible with regard to the temperature sweep direction[1]. This was a very unexpected result because many

[1] To the exclusion of cases in which there were two lines, $H_\perp$ and $H_\parallel$, observed simultaneously, and $H_\parallel$ had the same integral intensity as $H_\perp$. An abrupt magnetic cooling down to liquid nitrogen temperature occurs in such a case on cooling through T_H, which makes observation of the $H_\parallel$ line on cooling below T_H impossible.

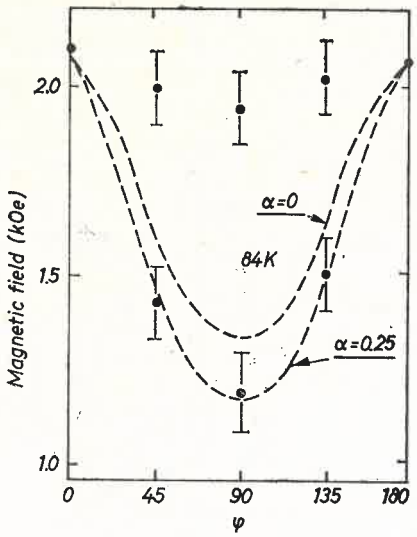

Fig. 6. Exemplifying angular dependence of the resonance fields in accordance with the results presented in figures 2 and 3. The broken lines approximate the theoretical dependence based on equations (2) for $\alpha = 0$ and $\alpha = 0.25$

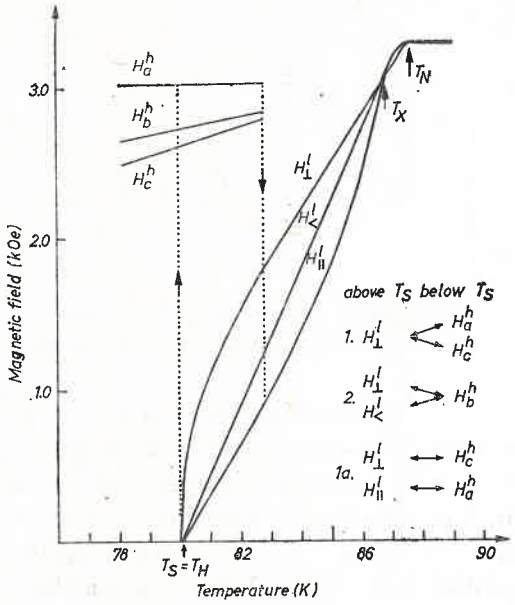

Fig. 7. Temperature dependence of the resonance fields after the sample damage by way of strong thermal variations or ionizing irradiation. The results are collected from two experiments; with magnetic field parallel to the ⟨100⟩ and ⟨110⟩ directions, respectively. In the former case the weak low-field line $H_\parallel^l$ arises from damage-induced domain with the easy axis in the initially "forbidden" direction (the correspondence of low-field to high-field lines for this case is listed at the point 1a). Hysteresis of this first-order structural phase transition is shown by dotted lines

authors estimated the typical first-order phase transition at about 81 K. In order to visualize such a phase transition in our experiments we made a search for the "better"samples. This search, however, failed of success. On the contrary, it was disclosed that our samples were of a much higher quality than was expected. When the samples were damaged by multiple, rapid and extending over a large range temperature variations (from 77 to 295 K), the different low-temperature behaviour was revealed. The results of AFMR measurements in such a case are collected in figure 7. The same behaviour as previously discussed was obtained on cooling the sample down to T_H, but just below this temperature a new group of resonance lines appeared at the higher field. We will call them the high-field lines to distinguish them from the former low-field lines; the resonance lines belonging to these groups will be designed by H^{h} and H^{l}, respectively. The correspondence between the low-field and the high-field lines is indicated in figure 7. The hysteresis of the undoubtedly first-order structural phase transition was about 3 K. The temperature of this transition will be designed by T_{S}.

More detailed measurements on the temperature dependence of the AFMR behaviour were made, especially near T_X and T_H. Additional investigations have been carried out in order to make clearer the relation between the structural and magnetic transitions. It is found that:

1) The domain distribution even in strongly damaged specimens was not homogeneous; two kinds of domains were always predominant.

2) There was no hysteresis effect discovered near T_X in spite of the high temperature resolution. In one sample, however, the same oscillatory behaviour as has been disclosed by Maartense and Searle [15] was observed.

3) In spite of many efforts no clear evidence of the magnetic phase transition at T_{S} was discovered. In only a few cases very weak additional resonance lines appeared which were not the lines arising from the uniaxial antiferromagnetic arrangement.

4) By exposing the single crystal to X-ray radiation prior to AFMR measurements, damaging effects analogous to those produced by rapid temperature variations were obtained. One difference, however, seems to be important: after the damage caused by ionizing radiation both the high-field and low-field phases coexisted in the sample near T_{S}. This was not observed otherwise.

5) If the sample, showing low-field-lines' behaviour only, was kept in a state of strong over-cooling at 77 K within several hours, the low-field lines were no longer observed below T_H; the structural phase transition appeared in the whole volume of the sample.

6) The changes in the crystal structure accompanying the phase transition at T_{S} were irreversible.

7) Very large heating or cooling effects accompanying the sample rotations against the magnetic field at each temperature but especially near T_H, was strongly anisotropic and dependent on the angle between the easy axis and the applied field. In extreme cases they led to abrupt cooling of the sample by several degrees. An analogous anisotropic dependence was discovered for the difference between the values of T_{N} and T_H. The absolute values of T_{N} and T_H was discovered to be strongly dependent on the sequence of the measurements previously performed on the given sample.

8) Owing to our experience with various doped $KMnF_3$ crystals it was established that any impurities in our samples, if they were in existance, had no observable influence on the AFMR results obtained.

9) The last of our observation worth noting is the linear increase of the anisotropy field H_A when the temperature is lowered between T_X and T_S. If one takes, according to Witt and Portis [29], the value of 8.68×10^5 Oe for the exchange field H_E, and assumes that it is constant with respect to temperature in the region considered, then the rate of increase of H_A between T_X and T_S is 0.65 Oe/deg.

5. *Discussion*

The AFMR behaviour displayed in figures 2 to 7 can be easily understood by using the schematic representation of the crystallographic and magnetic domains shown in figure 8. Here X, Y and Z refer to the laboratory coordinate system, and z_I and z_{II} are easy axes (the tetrad axes) of the domains I and II respectively, with the sublattice magneti-

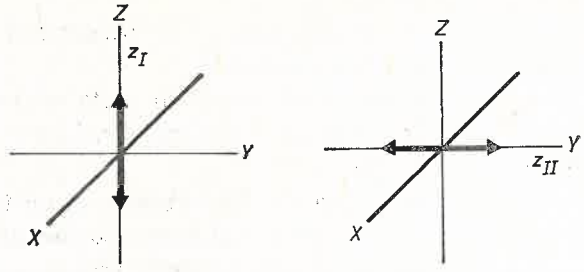

Fig. 8. Schematic representation of the crystallographic and magnetic domains for the discussion in Section 5

zations directed along each of them. The magnetic field can be aligned along any direction in the XY plane because the Z axis is the axis of sample rotation. Such a domain distribution as shown in figure 8 means that the distinguished direction in the sample due to crystallization is the X direction. Then if the magnetic field is directed, for example, along the X axis, the results are those shown in figure 2. On the other hand, if H is aligned along the XY diagonal one observes two low-field resonance lines $H^l_\perp$ and $H^l_<$ above T_S and only one high-field line $H^h_<$ below T_S (figure 7, case 2). It means that at T_S both the axes z_I and z_{II} twist in the X direction, i.e., in the previously "forbidden" direction.

As was pointed out in Section 4, in a strongly damaged sample it is possible to observe all three kinds of domains simultaneously, but the third domain always gives a resonance line of markedly lower intensity and, owing to this, such a domain can be easily distinguished (see for instance figure 7, case 1a).

From figures 3, 5 and 7 one can see that a common solution of the equations (2) exists at the temperature T_X. Thus we have $P = 0$ at T_X and also $H_A = 0$ at T_X. This means that the crystal lattice is exactly isotropic at this temperature. It is known that at the

temperature T_M (91 K) at which the M soft mode condenses, the lattice constant ratio is $c/a > 1$ [3]. Accordingly, one can immediately conclude that below T_X the structure must also be tetragonal but with this ratio reversed: $c/a < 1$. The structure must be of tetragonal symmetry because the crystal shows uniaxial antiferromagnetism below T_X. A consequence of the existence of the structure inversion at T_X is that the paramagnetic field H_p for the uniaxial antiferromagnetic phase below T_X is slightly lowered to below the high-temperature value of 3.3 kOe. The value of the applied field at T_X is 3.0–3.1 kOe and this is the value which should be taken into account when one resolves the equations (2). Let us designate the corrected paramagnetic field by H'_p; so $H'_p = H_{T=T_X}$.

With regard to the second common solution of equations (2) corresponding to $P = 1$ at T_H, it should be underlined that this temperature T_H depends on the resonance frequency and does not characterize any physical state of the crystal. However, due to the strong thermal effects connected with this temperature, at which the magnetic field approaches the zero value, an appearance of the first-order phase transition in this region is most probable at T_H precisely. Therefore, in our experiments we have observed that $T_S = T_H$ as is shown in figure 7. In agreement with our recent discussion the equality $P = 1$ means $H_{ef} = H'_p$ and not $H_{ef} = H_{p(T=295\,K)}$.

If the crystal undergoes the first-order structural phase transition at T_S then by using equations (2) and the results of the additional measurements of the resonance field anisotropy at 77 K [30] we can ascertain that the high-field lines apply to the same equations (2) as the low-field lines. Next, this means that the magnetic structure above and below T_S has the same uniaxial symmetry; the crystal is of tetragonal symmetry again. The new tetrad axis lying below T_S along the direction perpendicular to that one from the upper phase is at the same time the new easy axis for the magnetization of the domain under consideration. The only quantitative change at the phase transition, important for the AFMR, is the jump in the value of the anisotropy field H_A. By using equations (2) for the results above and below T_S one can see that H_A above T_S is four time as large as below T_S. A decrease in the anisotropy field means, of course, a less distorted perovskite-like structure. This is in agreement with crystallographic measurements at 50 K [3].

It is interesting to note that the common solution with $P = 0$ for the high-field lines seems to exist at the same temperature T_X as for the low-field lines. It is easily seen if one produces all high-field lines in figure 7 (or in figure 2c in reference [18]) to the higher-temperature region. This confirms our disclosure that $KMnF_3$ is uniaxial antiferromagnet below T_S too, if the applied field is not too high and the crystallographic domains are not very small. The relation of c/a and the direction of a change of the lattice parameters with temperature decreasing below T_S cannot be estimated from our experiments. However, it is well known [3] that the structure in the low-temperature region is quite similar to the ideal perovskite structure and that $c/a > 1$. Hence it is most natural to assume that the situation below T_S is analogous to that existing just below T_M(91 K), however, with a much weaker temperature dependence of the lattice parameters due to much smaller twisting of the octahedra.

On the other hand, it is known that if the applied magnetic field is of the order of 8 kOe, then the Curie temperature T_C equals T_S. The high-field lines apply in such a case

to resonance equations analogous to equations (2) deduced from conditions arising from the spin-flop phase; for comparison, one can see figure 2a in reference [18]. Very weak spin-flop high-field lines were observed in our experiments in those cases merely when very small (~ 10 μm) grains were left on the surface of the single-crystal sample. In such a case the spin-flop phase was extended on warming to the vicinity of T_N, as was pointed out by Maartense and Searle [15]. An estimation of the anisotropy field for the spin-flop lines gives one-half the value for the high-field, but not spin-flop lines. Such behaviour can be explained as follows. The smaller the given crystallographic domain is, the weaker the strain and the smaller the distortion are. If the size of the grain is smaller than a certain critical value, the first-order transition at T_S need not occur at all.

6. Concluding remarks

Our experiments allow several important conclusions concerning the crystal and magnetic structures of $KMnF_3$ single-crystal consisting of large crystallographic domains. Firstly, in the near vicinity of Néel temperature (at $T_X = T_N - 0.5$ K) the crystal lattice undergoes an inversion from the tetragonal phase with $c/a > 1$ to that phase of the same tetragonal symmetry, but with $c/a < 1$. The Néel temperature seems to be strongly connected with this inversion behaviour in the sense of the magnetoelastic coupling mechanism discussed by Maartense and Searle [15]. Secondly, in the vicinity of 81 K (at T_S) the crystal lattice undergoes a first-order structural phase transition to another tetragonal phase which seems to differ from the upper one in quantitative aspects only. It is discovered, however, that the structural phase below T_S strongly depends on the size of the crystallographic domains or, in other terms, on the strength of strains. If the crystallographic domains are not very large (with sizes not comparable to the volume of our sample) we can expect a transition to the orthorhombic phase at T_S instead of the new tetragonal one. The only difference in both cases concerns the new axis of rotations of the fluorine octahedra, MnF_6, below T_S. This new axis is perpendicular in both cases to the "old" axis of rotations above T_S — for instance, axis z_I (or z_{II}) in figure 8. When the new axis is directed along x_I or y_I axis, the structure below T_S also has tetragonal symmetry. If, however, the new axis is aligned along the $x_I y_I$ diagonal, the structure below T_S is orthorhombic rather than tetragonal[2]. Finally, the Curie temperature of transition to the weak-ferromagnetism phase is not necessarily equal to T_S. This transition seems to occur only if a stable crystallographic state with a spontaneous strain which can result in magnetic canting exists at low temperatures, below T_C. Thus we can suppose that the magnetic canting transition at T_C will occur only in small crystallographic domains, in which the orthorhombic structure exists below T_S; then T_C equals to T_S.

---

[2] In spite of the to some extent speculative character of the last conclusion, we can try to give a full description of all the structural phase transitions in a $KMnF_3$ crystal. Such a model based on that introduced by Hidaka [3] will be presented at the Eleventh International Congress of Crystallography, Warszawa, Poland, August 1978.

REFERENCES

[1] A. J. Heeger, O. Beckman, A. M. Portis, *Phys. Rev.* **123**, 1652 (1961).
[2] V. J. Minkiewicz, Y. Fujii, Y. Yamada, *J. Phys. Soc. Jap.* **28**, 443 (1970).
[3] M. Hidaka, *J. Phys. Soc. Jap.* **39**, 180 (1975).
[4] M. Hidaka, N. Ohama, A. Okazaki, H. Sakashita, S. Yamakawa, *Solid State Commun.* **16**, 1121 (1975).
[5] K. Gesi, J. D. Axe, G. Shirane, A. Linz, *Phys. Rev.* **B5**, 1933 (1972).
[6] S. M. Shapiro, J. D. Axe, G. Shirane, T. Riste, *Phys. Rev.* **B6**, 4332 (1972).
[7] D. J. Lockwood, B. H. Torrie, *J. Phys. C* **7**, 2729 (1974).
[8] D. J. Lockwood, G. J. Coombs, *J. Phys. C* **8**, 4062 (1975).
[9] V. V. Eremenko, V. J. Fomin, Y. A. Popkov, *Light Scattering in Solids*, M. Balkanski, R. C. C. Leite, S. P. S. Porto, *Flammarion Sciences*, Paris 1976, p. 905.
[10] M. Furukawa, Y. Fujimori, K. Hirakawa, *J. Phys. Soc. Jap.* **29**, 1528 (1970).
[11] W. D. McCormick, K. J. Trappe, *Low Temperature Physics — Lt 13*, Eds K. D. Timmerhaus, W. J. O'Sullivan, E. F. Hammel, Plenum Press, New York, London 1974, Vol. 2, p. 360.
[12] J. J. Martin, G. S. Dixon, P. P. Velasco, *Phys. Rev.* **B14**, 2609 (1976).
[13] B. Okai, J. Yoshimoto, *J. Phys. Soc. Jap.* **39**, 162 (1975).
[14] E. Strauss, H. J. Riederer, *Solid State Commun.* **21**, 429 (1977).
[15] I. Maartense, C. W. Searle, *Phys. Rev.* **B6**, 894 (1972).
[16] I. Maartense, *Solid State Commun.* **12**, 1133 (1973).
[17] F. Borsa, *Phys. Rev.* **B7**, 913 (1973).
[18] K. Saiki, *J. Phys. Soc. Jap.* **33**, 1284 (1972).
[19] K. Saiki, K. Horai, H. Yoshioka, *J. Phys. Soc. Jap.* **35**, 1016 (1973).
[20] K. Saiki, H. Yoshioka, *Solid State Commun.* **15**, 1067 (1974).
[21] K. Aso, *Jap. J. Appl. Phys.* **15**, 1243 (1976).
[22] D. J. Benard, W. C. Walker, *Rev. Sci. Instrum.* **47**, 122 (1976).
[23] O. Beckman, K. Knox, *Phys. Rev.* **121**, 376 (1961).
[24] A. Chełkowski, P. Jakubowski, D. Kraska, A. Ratuszna, W. Zapart, *Acta Phys. Pol.* **A47**, 347 (1975).
[25] A. Ratuszna, *Thesis*, Katowice 1978 (in Polish).
[26] T. Nagamiya, K. Yoshida, R. Kubo, *Adv. Phys.* **4**, 1 (1955).
[27] S. Foner, *Phys. Rev.* **130**, 183 (1963); and *Magnetism*, Eds G. T. Rado and H. Suhl, New York 1963, Vol. I, p. 383.
[28] A. J. Heeger, A. M. Portis, D. T. Teaney, G. Witt, *Phys. Rev. Lett.* **7**, 307 (1961).
[29] G. L. Witt, A. M. Portis, *Phys. Rev.* **135**, A1616 (1964).
[30] P. Jakubowski, *Thesis*, Katowice 1976 (in Polish).